Received: 31 March 2011 ■ *Revised: 16 June 2011* ■ *Accepted: 20 June 2011* ■ *Publication: 1 July 2011*

EJMS EUROPEAN JOURNAL OF MASS SPECTROMETRY

IYC 2011 International Year of CHEMISTRY

OPEN ACCESS

Review

Some thoughts on electrospray ionization mechanisms

Sara Crotti,[a] Roberta Seraglia[b] and Pietro Traldi[b,*]

[a]Department of Environmental Sciences, Informatics and Statistics, Cà Foscari University, 2137 Dorsoduro, Venice, Italy

[b]CNR-ISTM, Corso Stati Uniti 4, I-35127 Padova, Italy. E-mail: pietro.traldi@adr.pd.cnr.it

Electrospray ionization (ESI) mechanisms are highly complex, due to a series of physical and chemical phenomena taking place on a complex system, as a solution is. In fact, even if the solution of an analyte in a protic medium can be considered at first sight to be a two-component system, the presence of solvent dissociation equilibria and the possible interactions solvent–solvent dissociation products, solvent dissociation products–analyte make this system highly complex, also for the presence of possible ionic compounds (for example, Na^+, K^+) which strongly affect the above equilibria. A high number of research articles have been published, mainly devoted to charged droplet production and to gas-phase ion generation. They all show the high complexity of the processes affecting electrospray measurements related to either the chemical equilibria present in the condensed phase and to electrolysis processes at the emitter tip or to the processes occurring in the sprayed droplets. As a result, the chemical composition inside the small droplets from which the analyte ions are generated can be significantly different from those in sprayed solution. In this review, after a short survey of the proposed ESI mechanisms, some experiments are described. They were performed to examine if ion mobility in solution, before the formation of the sprayed charged droplets, can affect the ESI results. The data, obtained by studying both inorganic and organic analytes, indicate that the ESI spectra are dependent on the analyte dimension and charge state which, as a consequence, affect their ion mobility in solution.

Keywords: electrospray ionization, ion mobility, review

Introduction

Electrospray (ESI) mass spectrometry is surely one of the most employed analytical techniques, due to its wide applicability and to the valid results obtained in the biomedical field.[1] This success is mainly due to easy coupling with liquid chromatography and electrophoretic separation devices, but also on its ability to detect both small (for example drug metabolites) and large (for example, proteins, peptides, oligonucleotides) molecules. Furthermore, it is an effective chemico–physical tool in the study of non-covalent interaction, being able, in some cases, to transfer non-covalent complexes present in solution into the gas phase without disrupting the non-covalent interaction.

Its importance was recognized by awarding the Nobel Prize, in 2002, to John Fenn for the development of ESI.[2] He died on 10th December 2010, but his spirit will survive in our laboratories, where ESI represents one of the most employed techniques to characterize, from the structural point of view, not only biomolecules (proteins, peptides and nucleic acids), but also organometallic and inorganic compounds, as well as polymers.

The production of analyte ions, starting from their solution, is highly complex, due to the occurrence of synergic chemical and physical phenomena. Unfortunately, what is often observed in many labs is that ESI is considered only as a very

ISSN: 1469-0667
doi: 10.1255/ejms.1129

effective "black box". The marketing tends to present ESI as a technique which one does not need to know *how* it works and which can easily be managed by suitable operative software. In some cases, ESI/MS is described as a LC detector, among those (ultraviolet, diode-array detector, fluorimetric) usually employed in LC analyses. This is surely the reason for the wide scope of ESI but it is, in our opinion, a very restrictive view which does not make the users aware of all aspects (either positive or negative) which are the basis of the analytical procedure.

The tendency is often just to consider the ESI/MS system not as a mass spectrometric device but just the screen and the keyboard of a data system linked to the instrument. Sometimes, we have been given the impression that at the beginning of experimental theses, our students considered the ESI/MS system to be similar to a computer game. So, the knowledge of ESI mechanisms is essential and, in this respect, the recent exhaustive review from Kebarle and Verkerk, entitled "Electrospray: from ions in solution to ions in the gas phase, what we know now", covers all the aspects of ESI described by different authors over recent years.[3] The different sections of the review related to the formation of gas-phase ions (major stages in ESI, generation of the charged droplets at the ESI capillary tip, electrospray as a special electrolytic cell, required electrical potential for ESI which can cause electrical discharges etc.) allow readers to gain a wide understanding of what happens inside an ESI source.

The present paper reports, in the introduction section, on some fundamental aspects, widely described and discussed in the literature, of what happens to an analyte solution during the electrospray formation and inside the droplets. In the results and discussion section, some considerations of what happens inside the spraying capillary and how these hypotheses fit with the experimental data are made. As will be described, the experiments indicate that the ion mobility of analytes in the original solution can play some role in the obtained ESI data.

Fundamental aspects of ESI-MS

The production of charged droplets is a natural phenomenon, the final product of which we observed the first time we looked at a cloudy sky. The interaction of small water droplets with the electrical fields between clouds and earth leads to the formation of charged droplets, which precipitates storms and hail.

The first experiments on electrospray were thought to be those carried out by Abbé Jean-Antoine Nollet, who observed, in 1750, the aerosol formation when water flowed from a small hole present in an electrified metal vessel when a grounded metallic bar was placed close to it. Some further experiments (which nowadays seem to be quite strange) were performed on a physiological level. Abbé Nollet observed that "a person, electrified by connection to a high voltage generator (hopefully well insulated from the ground!—authors' note) would not bleed normally if he was to cut himself; blood sprayed from the wound".[4] This result was in agreement with the science of that time, considering physics, chemistry, physiology, medicine and religion as different view of the same reality.

About a century later, Lord Kelvin studied the charging between water dripping from two different liquid nozzles, which leads to the electrospray phenomena at the nozzles themselves.[5] In the 20th century, a series of systematic studies on electrospray were carried out by Zeleny,[6] Wilson and Taylor[7,8] and, in the middle of the century, electrospray was widely employed as an effective painting technique, applied to vehicles, household goods and various metal objects.[9,10]

Electrospray became of analytical interest in 1968, when Dole and co-workers produced gas-phase, high molecular weight polystyrene ions by electrospraying a benzene/acetone solution of the polymer.[11]

The early studies of Yamashita and Fenn[2] brought electrospray to the analytical world and from then electrospray applications have shown fantastic growth. This technique can be considered the ionization method which the whole scientific community was waiting for; an effective and valid approach for the direct study of analytes present in solution and, consequently, easy coupling with LC methods. Furthermore, the behavior of proteins and peptides (as well as oligonucleotides) in electrospray conditions, leading to the production of multiply charged ions, makes this ionization method essential in biomedical studies and in proteome investigations without the need of a mass analyzer exhibiting high mass range (i.e. time-of-flight); however, in this case high resolution is needed.

The instrumental set-up for electrospray ionization experiments is schematized in Figure 1. The solution is injected through a stainless steel capillary (10^{-4} m o.d.). Between this capillary and a counter electrode, placed at a distance in the range 3–10 mm, a voltage of some kV is applied. In these conditions, what is observed is the formation of a solution cone just outside the capillary. The formation of this cone-shaped structure can be justified by the action of charged species present in the solution under the electrostatic field existing between the capillary and the counter electrode.

After cone production, for high enough applied electrical fields, the formation of droplets from the cone apex are observed, which further migrate, due to their charge, through the atmosphere to the counter electrode.[7]

It has been proved that droplet formation is strongly influenced by: voltage applied between capillary and counter electrode; solvent chemical–physical characteristics (viscosity, surface tension, pK_a); concentration of ionic analytes and concentration of inorganic salts.

In the case of positive ion analysis, the capillary is placed at a positive voltage while the counter electrode is placed to a negative voltage (as shown in Figure 1). The opposite is used for negative ion analysis. As a result of this phenomenon, the generated droplets carry a high number of positive (or negative) charges. This behavior can be enhanced by the use of a coaxial nitrogen gas steam and this is the instrumental

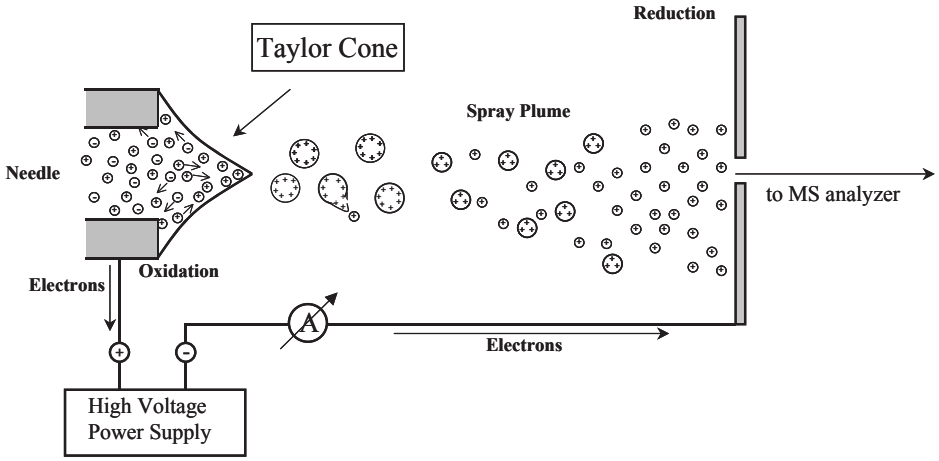

Figure 1. Instrumental set-up for electrospray experiments in positive ion mode. Adapted with permission from *Anal. Chem.*, Blades, Ikonomou, Kebarle (Reference 12). Copyright 1991 American Chemical Society.

set-up usually employed in commercially available electrospray sources.

The processes which lead to a deep change in composition of ions in the spray solution are those occurring at the metal–liquid capillary interface, where oxidation reactions take place.[12] They were studied using a Zn capillary tip. This experiment was performed by employing three different spraying capillary structures. The stainless steel capillary normally employed (sometimes covered by a platinum layer but passivated anyway by the presence of a thin layer of chrome oxides) was substituted by one with a tip made with Zn. Zn was chosen as a suitable material, as it has a very low reaction potential.

$$Zn_{(s)} \rightarrow Zn^{2+} + 2e \qquad \text{with } E^{\circ}_{red} = -0.76\,V$$

Under these conditions, Zn^{2+} ions were easily detected in the mass spectrum, simply by spraying methanol at a flow rate of $20\,\mu L\,min^{-1}$. In order to be confident of the production of Zn^{2+} at the capillary tip, and to exclude other possible origins, a further experiment was carried out, placing the Zn capillary before the electrospray capillary line and electrically insulated from it. Under these conditions Zn^{2+} ions were not detected. These results provide good evidence that electrochemical oxidation takes place at the liquid–metal interface of the electrospray capillary tip.

It can therefore be considered that the spraying capillary tip and the entrance capillary port at the counter electrode constitute an electrolysis cell. In the case of positive ion analysis, the electrochemical oxidation reaction would occur at the liquid–metal interface of the capillary tip and the yield of this reaction would depend on the electrical potential as well as on the electrochemical oxidation potentials from the different possible reactions. Kinetic factors can only exhibit minor effects, considering the low current involved.

The effect of oxidation reactions at the capillary tip will be the production of an excess of positive ions, together with the production of an electron current flowing through the metal (see Figure 1). The excess of positive ions could be the result of two different phenomena, i.e. the production of positive ions themselves or the removal of negative ions from the solution.

The electric current, due to the motion of the droplets, measured by the amperometer (A) shown in Figure 1, is surely a parameter of interest, allowing for the estimation of the total number of elementary charges leaving the capillary which, theoretically, could correspond to gas-phase ions. The droplet current, I, the droplet radii, R, and charge, q, were originally calculated by Pfeifer and Hendricks;[13] more recently, de la Mora and Locertales[14] found, based on both theoretical calculation and experimental data, the following equations for the same quantities:

$$I = f\left(\frac{\varepsilon}{\varepsilon_0}\right)\left(\gamma K V_f \frac{\varepsilon}{\varepsilon_0}\right)^{\frac{1}{2}} \tag{1}$$

$$R \approx \left(\frac{V_f \varepsilon}{K}\right)^{\frac{1}{3}} \tag{2}$$

$$q = 0.7\left[8\pi\left(\varepsilon_0 \gamma R^3\right)^{\frac{1}{2}}\right] \tag{3}$$

where γ is the surface tension of the solvent; K is the conductivity of the infused solution; ε is the dielectric constant of the solvent; ε_0 is the dielectric constant of the vacuum; V_f is the flow rate and $f\left(\frac{\varepsilon}{\varepsilon_0}\right)$ is a function of the $\varepsilon/\varepsilon_0$ ratio.

Equation (1) shows the dependence of I from the two most relevant experimental parameters, i.e. the flow rate (V_f) and the conductivity (K). Equation (3) shows a decrease in the dimension of the droplets by increasing the solution conductivity.

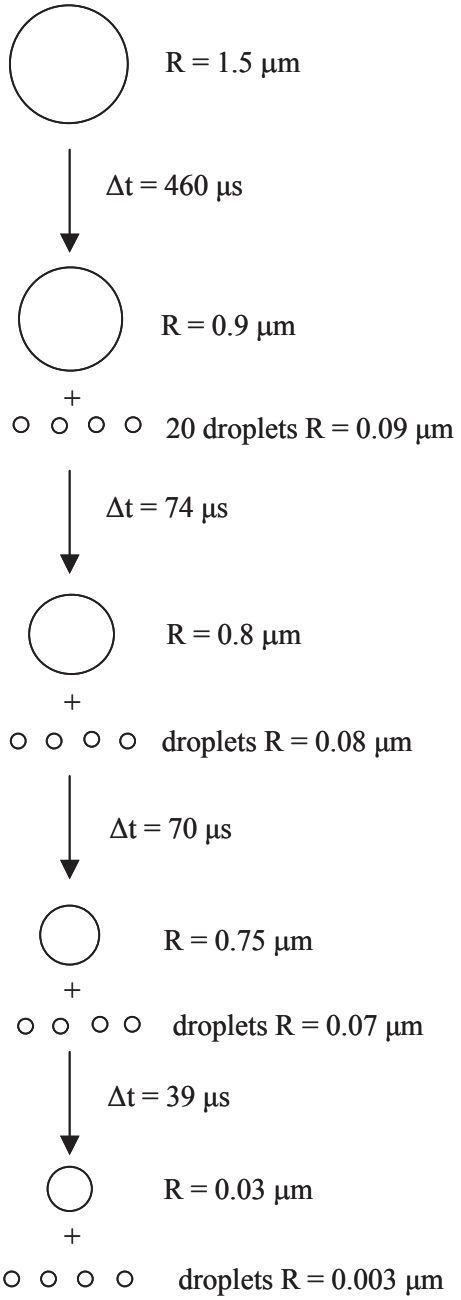

Figure 2. Theoretical calculation of droplets dimension and life times. Reprinted from *J. Am. Soc. Mass Spectrom*. Volume 15, M. Peschke, U.H. Verkerk and P. Kebarle, "Features of the ESI mechanism that affect the observation of multiply charged noncovalent protein complexes and the determination of the association constant by the titration method", 1424 Copyright 2004 with permission Elsevier.

These relationships are particularly relevant because in solution, when different electrolytes are present, the conductivity, K, may be obtained as the sum of the conductivities due to the different species and is proportional to the ion concentration:

$$K = \sum_i \lambda_{0,m,i} C_i \quad (4)$$

where $\lambda_{0,m,i}$ is the molar conductivity of the electrolyte i.

The charged droplets, generated by solution spraying, decrease their radius due to solvent evaporation but their total charge amount remains constant. The energy required for the solvent evaporation is, in a first step, due to environmental thermal energy. In a second step, this process is enhanced through further heating obtained with a heated entrance capillary or by collisions with heated gas molecules. The maintenance of the total charge during this evaporation phase can be explained by the fact that the ion emission from the solution to the gas phase is an endothermic process. The decrease in the droplet radius can be described by Equation (5) where $\bar{\nu}$ is the average thermal speed of solvent molecules in the vapor phase:

$$\frac{dR}{dt} = -\frac{\alpha \bar{\nu}}{4\rho} \frac{p^0 M}{R_g T} \quad (5)$$

where p^0 is the solvent vapor pressure at the droplet temperature; M is the solvent molecular weight; ρ is the solvent density; R_g is the gas constant; T is the droplet temperature and α is the solvent condensation coefficient.

This relationship demonstrates all the factors that can influence the droplet dimensions and, consequently, the effectiveness of ESI.

The decrease in the droplet radius with respect to time necessarily leads to an increase in the surface charge density. When the radius reaches the Rayleigh stability limit [given by Equation (6)], the electrostatic repulsion is identical to the attraction due to surface tension. For lower radii, the charged droplet is unstable and decomposes through a process generally defined "Coulombic fission".[15]

$$q_{R_y} = 8\pi \left(\varepsilon_0 \gamma R^3\right)^{\frac{1}{2}} \quad (6)$$

Peschke *et al.*[16] calculated the lifetime, dimension and fragmentation of droplets (see Figure 2).

Until now, two different theories have been proposed to give a rationale for the formation of ions from small charged droplets. The first of these has been described by Cole[17] and Kebarle & Peschke[18] as a series of scissions which lead, at the end, to the production of small droplets bringing one or more charges but only one analyte molecule. When the last few solvent molecules evaporate, the charges are localized on the analyte, giving rise to the most stable ions in the gas phase. This model is usually called "the Charged Residue Mechanism" (CRM) (see upper part of Figure 3).

Thomson and Iribarne[19] proposed a different mechanism, in which a direct emission of ions from the droplet is considered. It occurs after the droplets have reached a critical radius. This process is called "Ion Evaporation" (IEM) and is thought to be dominant with respect to Coulumbic fission from particles with radii $r < 10$ nm (see lower part of Figure 3).

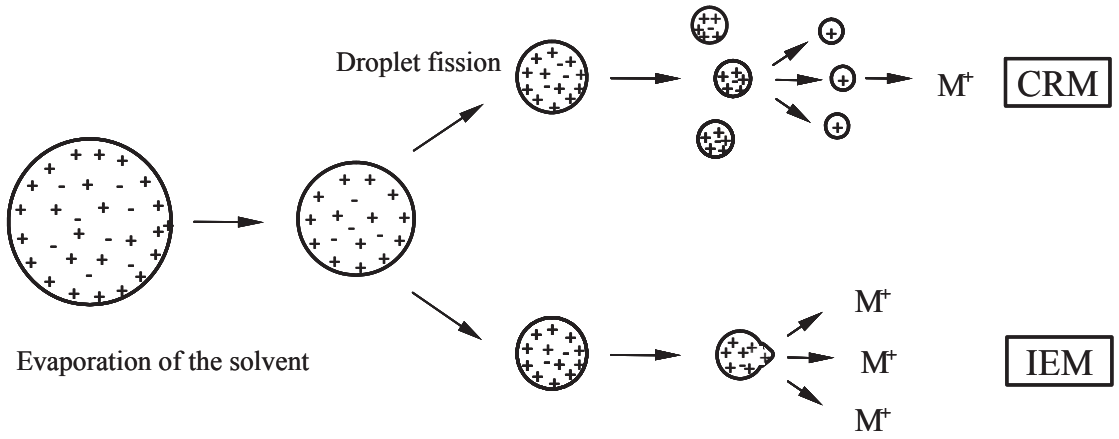

Figure 3. Schematic description of the charged residue (CR) and ion evaporation (IE) mechanisms.

Both CRM and IEM can be invoked to explain many of the behaviors observed in ESI experiments. However, a clear distinction between the two mechanisms lies in the way in which an analyte molecule is separated from the other molecules (either of analyte or solvent present in droplets). In the case of IEM, this separation takes place when a single analyte molecule, bringing a part of the charge in excess of the droplet, is desorbed in the gas phase, reducing the coulombic repulsion of the droplets. Using the CRM mechanism, this separation occurs through successive scissions, reducing the droplet dimensions until only one single molecule of analyte is present. In general, the CRM model is considered valid in the process of gas-phase ion formation for high molecular weight molecules.

CRM and IEM mechanisms consider the behavior of a charged droplet in a free space, in which no electrical field is present. In contrast, in an ESI source, a strong electrical field is present, originating from the voltage applied to the spraying capillary. Zhou and Cook[20] studied the effects of ion pairing, surface activity and electrophoretic mobility, which can affect the surface concentration of ions in the electrosprayed droplets.

Some theoretical considerations indicate that for ionic species under the effect of strong electrical fields (in the range 10^6–10^7 V m^{-1} at the ES capillary tip), electrophoretic migration is responsible for mass transport, the initial charge separation and the emission of charged droplets. Once the droplet is emitted from the apex of the Taylor cone, as described above, the excess of cations (in positive ion mode) will distribute on the surface. However, in the presence of the applied field, it will penetrate inside the droplet and will induce an axial charge separation, due to electrophoresis occurring inside the droplet. The amount of axial charge separation will be related to the externally applied electrical field and, if the migration rates allow, some inhomogeneous distribution of both cations and anions may result from their differential electrophoretic migration. This aspect can be described by Figure 4. The more mobile species may become enriched in the small offspring droplets *"if the applied field remains adequate to maintain some charge separation at least until the initial Rayleigh subdivision"*.[20]

It must be considered that the field experienced by the droplet is not constant, but decreases from the spray

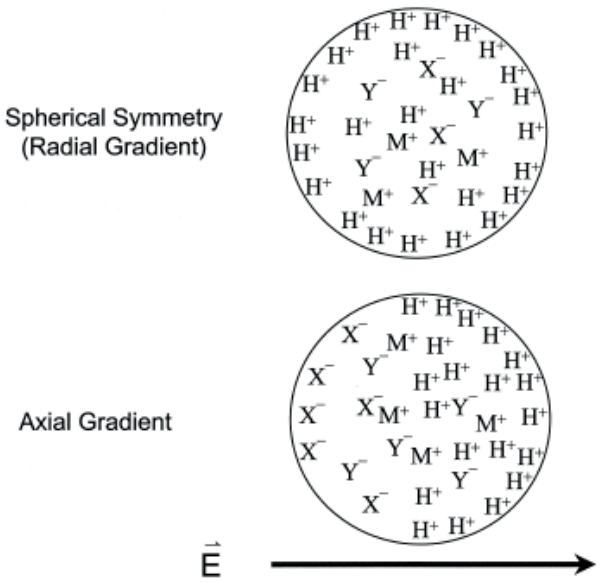

Figure 4. Exaggerated cartoon showing the radial charge gradient derived from the mutual coulombic repulsion among excess charges in the droplet (resulting in a spherically symmetric self-developed field with no net field at the droplet center) and the axial charge gradient that may develop via electrophoretic charge separation in response to the externally applied field. The case shown is for positive ion mode (excess of positive charge, here attributed to electrophoretically generated protons). M^+ and Y^- are arbitrary ions of mobility less than H^+ and X^-. With kind permission from Springer Science + Business Media, *J. Am. Soc. Mass Spectrom.*, "A mechanistic study of electrospray mass spectrometry: charge gradients within electrospray droplets and their influence on ion response", Volume 12, 2001, page 206, S. Zhou and K.D. Cook, Figure n.1.

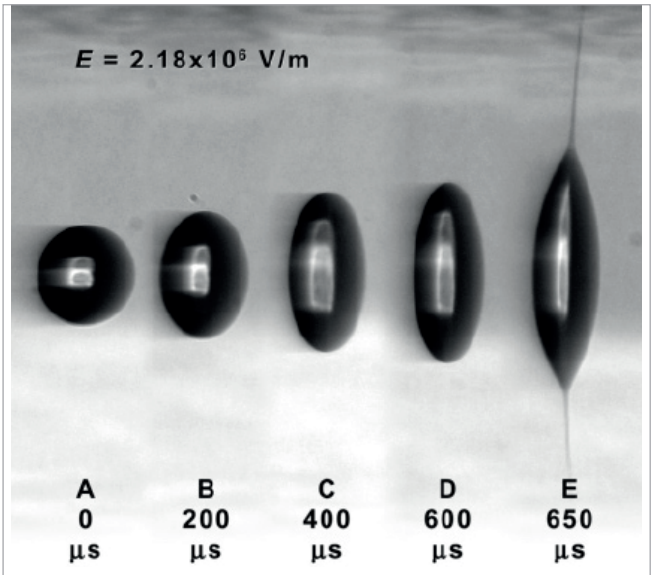

Figure 5. Sequences of 225 µs droplets exposed to an electric field for the indicated time period. Frames A-E represent droplets in a 2.18×10^6 V m^{-1} field. The sequence is characterized by symmetrical elongation as exposure to the field increases, culminating in the formation of two conical tips and oppositely charged progeny jets characteristic of FIDI. At 2.18×10^6 V m^{-1}, FIDI develops after 650 µs in frame E. Reprinted with kind permission from R.L. Grimm and J.L. Beauchamp, "Dynamics of field-induced droplet ionization: time-resolved studies of distorsion, jetting and progeny formation from charged and neutral methanol droplets exposed to strong electric field", *J. Phys. Chem. B* 109, 8244 (2005). Copyright 2005, American Chemical Society.

capillary to the entrance capillary and, consequently, the sprayed droplets will interact with the strongest field. Just to have a general view, a small ion (alkali cation) would take 94–940 µs to migrate from the center to the surface of a droplet which had just been sprayed ($R = 1.5$ µm, see Figure 2) and 8–80 µs to reach the surface of an offspring droplet ($R = 0.08$ µm). These time values indicate the feasibility of some axial charge separation.

The charge separation phenomena has recently been described and studied in detail by Grimm and Beauchamp.[21] They showed that strong electrical fields are able to extract positive and negative ions directly from a *neutral* droplet by studying the droplet behavior under and over the Tailor limit, defined as

$$E_c^0 = \frac{c}{(8\pi)^{1/2}} \left(\frac{2\sigma}{\varepsilon_0 r} \right)^{1/2}$$

(the constant, c, has been determined both empirically and theoretically; σ is the surface tension and r is the droplet radius).

When a droplet is placed in fields $E < E_c^0$, it undergoes damped oscillations, the frequency of which is related to the E value. These oscillations are due to a first phase of charge separation, followed by the restoration of the initial charge distribution, due to attractive forces among the initially separated charges.

For $E > E_c^0$, the process called field-induced droplet ionization (FIDI) takes place and is well described by photographs reported in Figure 5. The originally spherical droplet, after 400 µs, distorts into prolate ellipsoids. The sequence in Figure 5 shows the symmetrical elongation with the formation of two conical tips and the oppositely charged progeny jets. The experimental data allowed a droplet stability diagram to be obtained, relating the applied field, E, to the charge, q, (Figure 6). It enables *neutral* as well as charged droplet behavior to be described.

Analogous phenomena were observed by Gomez and Tang[22] for heptane droplets generated in electrospray conditions. The Coulombic fission was captured in microphotographies showing the droplet with one or two diametrically opposed protrusions terminating in the ejection of smaller offspring.

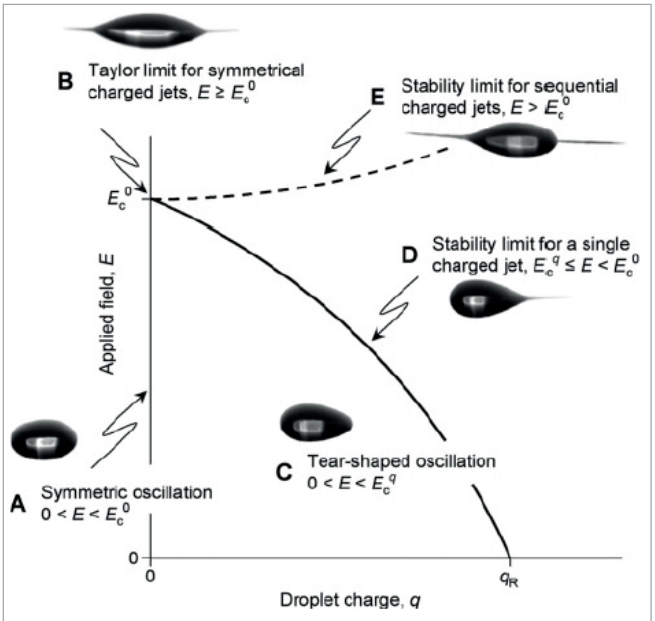

Figure 6. Summary of droplet stability as a function of net charge and applied electric field. Uncharged droplets below the critical field E_c^0 (A) undergo symmetric shape oscillation. Above E_c^0, uncharged droplets above E_c^0 symmetrically elongate and simultaneously emit positive and negative progeny jets (B). The critical field for progeny formation from charged droplets decreases with increasing charge, represented by E_c^q (solid curve). Below E_c^0, charged droplets oscillate with asymmetric, tear shapes (C). Above E_c^q, droplets emit a single jet of charged progeny (D). At fields greater than E_c^0, a second field exists above which charged droplets emit sequential jets (E). The curve of this stability limit is unknown and resented with a dashed line. Reprinted with kind permission from R.L. Grimm and J.L. Beauchamp, "Dynamics of field-induced droplet ionization: time-resolved studies of distorsion, jetting and progeny formation from charged and neutral methanol droplets exposed to strong electric field", *J. Phys. Chem. B* 109, 8244 (2005). Copyright 2005, American Chemical Society.

Both the data of Gomez and Tang[22] and those of Grimm and Beauchamp[21] indicate the capability of an electrical field to activate charge separation phenomena in either charged or *neutral* droplets, so supporting the findings of Zhou and Cook.[20]

Most of the research on ESI mechanisms has been devoted to the description of how gaseous ions are generated from the sprayed solution of the analyte.[3] We focus our attention on what happens inside the spraying capillary, due to electrical field penetration. Different analytes with different charge state and/or dimension will move, inside the solution, in the direction of the electrical field and, consequently, their ion mobility should, in principle, play a role. Some experiments were performed to verify this hypothesis and here we report and discuss the data obtained.

Experimental

NaCl, KCl, RbCl and $AlCl_3$ were purchased from Carlo Erba (Milan, Italy); CsCl was purchased from Riedel-de Haën AG (Hannover, Germany); Horse Heart Cytochrome *C* (Cyt*C*), Angiotensin II and 1,6-dimethyl-4-hydroxy-3-pyridincarboxilic acid were purchased from Sigma–Aldrich (Milan, Italy).

ESI-MS analysis was performed with an LCQ DECA (Thermo Fisher, Rodano, Milan, Italy), operating in the positive ion mode. Sheath gas and auxiliary gas flow rate were 50 and 5 (arbitrary units), respectively and entrance capillary temperature was set at 280°C. For alkali ion solution analysis, the RF injection parameter was kept at 20 to avoid the low mass cut off for Na^+ ions, while for the other analyses it was kept 30.

NanoESI analysis was performed on a Q-TOF G6520 instrument (Agilent Technologies Inc., Santa Clara, CA, USA), equipped with an Agilent HPLC-Chip/MS interface. For this investigation, a G4240-61015 infusion chip was used and the Cyt*C* solution (10^{-5} M in deionized water) was infused by a syringe pump at a flow rate of 18 μL h^{-1}. The mass spectrometric conditions employed were as follows: positive ion mode; V_{cap}: 1900–1720 V; drying gas flow rate: 4 L min^{-1}; drying gas temperature: 320°C; fragmentor voltage: 200 V; skimmer voltage: 65 V; reference masses: *m/z* 149.02332 and *m/z* 1221.02332.

Alkali metal (Na, K, Rb and Cs) chlorides were mixed in equimolar ratio and diluted in deionizer water to obtain a 10^{-5} M working solution. The alkali metals solution was analyzed as it was and after a 1 : 1 mixture whith 10^{-5} M Angiotensin II solution. Cyt*C* was solubilized in deionized water to obtain a 10^{-5} M solution before ESI-MS analysis.

$AlCl_3$ and 1,6-dimethyl-4-hydroxy-3-pyridincarboxilic acid (L) were dissolved in deionized water to obtain a concentration of 10^{-5} M with a molar ratio Al/L of 1 : 3. The ESI-MS conditions were those already described. Potenziometric analysis of the same solution was performed by a HI 9017 pH meter (Hanna Instruments Inc., Rhode Island, USA) equipped with a Crison 5081 glass electrode (pH range: 0–14).

Results and discussion

On the solution inside the spraying capillary

If pure water is flowing inside the spraying capillary, it must be considered that hydronium (H_3O^+) and hydroxy (OH^-) ions are present and that $K_w = 10^{-14}$ at 25°C. It means that in pure water H_3O^+ and OH^- ions are present in an homogeneous concentration of 10^{-7} M. Of course, in the absence of any electrical field, the equilibrium:

$$H_2O + H_2O \leftrightarrows H_3O^+ + OH^-$$

is constant but, in the presence of an electrical field, ion mobility phenomena take place, leading to an inhomogeneous distribution of charged species. If an ion is subjected to the electrical force $F_e = zeV/l$ and the friction force is $F_f = 6\pi r\eta v$, at the stationary state $F_e = F_f$, i.e.

$$v = zeV/6\pi r\eta l \quad (7)$$

For a singly charged ion of 1 nm of mean radius in aqueous solution, which experiences the potential $V = 4$ kV, the related speed is

$$v = 3.4\ \text{cm s}^{-1}.$$

The electrical field, (E_c), experienced by the ion inside the final part of the spraying capillary, placed at a voltage, *V,* has been calculated by Loeb[23]

$$E_c = 2\ V_c/[r_c\ ln(4d/r_c)] \quad (8)$$

where: V_c is the applied potential; r_c is the outer radius of the capillary and *d* is the capillary tip–counter electrode distance.

It should be noted that, in this formula, the two most relevant terms are the voltage applied to the spraying capillary (V_c, linearly related to the field) and the radius of the spraying capillary (r_c, inversely related to the field). In contrast, the distance, *d*, between the spraying and entrance capillaries plays only a limited role, being under a logarithm.

If we consider a water flow of 10 μL min^{-1} in a capillary with an inner section of 0.028 mm^2, the mean axial speed results in:

$$v_f = 6.1\ \text{cm s}^{-1}.$$

This must be considered the mean speed because of the nature of the laminar flow (see Figure 7) and the speed distribution [$v(r)$] which can be calculated as:

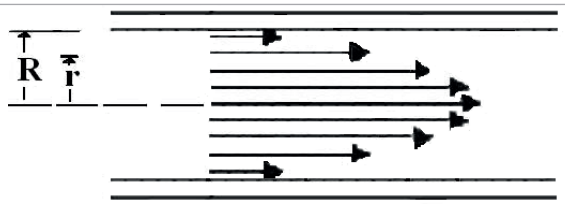

Figure 7. Speed distribution in laminar flow regime.

$$v(r) = v_m (1 - r^2/R^2) \quad (9)$$

where: v_m is the mean speed (calculated from the flow rate); r is the radial distance from the capillary axis and R is the capillary internal radius. It will be zero on the capillary wall and its maximum value will be along the capillary axis.

In the absence of any electrical field, H_2O, H_3O^+ and OH^- will experience the same speed distribution. If a strong positive potential is applied on the capillary wall, the situation necessarily shows a deep change. In this case, due to the field penetration, inside the capillary two different parallel speeds are experienced by the flowing ions: that due to the selected flow rate (axial) and that due to ion mobility (axial).

In presence of a positive potential, all the negatively charged species will be attracted to the capillary wall, while the positively charged ones will be concentrated along the capillary axis, i.e. in the region of the highest axial speed.

Then, along the capillary axis, a high density of H_3O^+ ions will appear with the consequent decrease in pH value. When a neutral analyte, M, is present in a water solution, it will experience a high acidity region in the terminal part of the capillary, reflecting in the production of a high yield of MH^+. Another aspect to be considered is the polarity of neutral water molecules which will lead to the interaction of the partial negative charge present on the oxygen atom with the capillary wall, leading to more acidic water molecules, which are responsible for a more effective production of H_3O^+.

These results, in particular the clear increase in H_3O^+ concentration in the axial region of the capillary, are in agreement with the findings of Rellán-Álvarez *et al.*,[24] showing a decrease in the pH of 1–2 units with respect to that of the original solution. These decreases can also be related to the increase in H_3O^+ concentration in the sprayed droplet during the solvent evaporation phase, but the original H_3O^+ concentration in the ejected droplet is strongly related to the H_3O^+ concentration in the Taylor cone.

Furthermore, it must be considered that the H_3O^+ concentration in the axial part of the spraying capillary will necessarily be the expression of an equilibrium, due to space charge effects. In other words, the pH value will decrease until a minimum value is reached, under which repulsive phenomena will take place. This hypothesis is in agreement with the results obtained by Tang and Kebarle[25] in the study of the ion intensity of an ionic analyte (Bu_4N^+), as well as of protonated codeine (MH^+), by varying their concentration. In both cases, a plateau is reached for concentration of about 10^{-5} M. In the case of Bu_4N^+, by increasing the concentration no more ions can be focused in the terminal part of the capillary along the axial direction, while for codeine, the limit of H_3O^+ concentration is responsible for the observed behavior.

Again, it must be considered that the axial region of the final part of the spraying capillary represents, as discussed above, the region of highest linear speed, due to the laminar flow regime.

Coming back to H_2O, H_3O^+ ions will be concentrated along the final part of spraying of the capillary axes and, consequently, a high concentration of H_3O^+ will reach the meniscus at the end of the capillary, so generating the Taylor cone responsible for the charged droplets production. It is interesting to observe that the electrical field experienced on the top of the Taylor cone has been calculated to be in the order of 10^8 V cm^{-1}, the same as are present in FI/FD conditions.[26]

Axial ion mobility effects

The electrical field, due to the voltage between spraying and entrance capillaries, is responsible for the formation of the Taylor cone, but will also penetrate either in the Taylor cone or inside the spraying capillary due to the presence of ions. Its strength will depend on geometrical factors as well as on the dielectrical constant of the sprayed solution. Its effect necessarily influences the mobility of the ions inside the solution, the velocity of which can be approximately defined by Equation (7). This equation shows that the speed of an ion depends directly on the number of charges (ze) and inversely on its dimension (r).

It would therefore be expected that ions of different m/z ratios and/or different cross sections would exhibit different speeds. Consequently, for ions already present in the sprayed solution, a discriminatory effect would be present when a potential was applied to the spraying capillary. To evaluate this effect some experiments were carried out.

First, an equimolar solution of Na^+, K^+, Rb^+ and Cs^+ ions was analyzed by spraying it at different voltages, V. For $V = 0.5$ kV, no electrospray phenomenon can take place. In fact, the Smith [27] approximate equation for the potential required for the onset of ESI

$$V_{on} = (r_c \gamma \cos\alpha / 2\varepsilon_0)^{1/2} \ln(4d/r_c) \quad (10)$$

shows that the V_{on} value, calculated for a spray tip of 0.1 mm radius and a distance, d, between spraying and entrance capillaries of 4 cm, is for water about 4 kV.

Table 1. Ionic radii, enthalpy of hydration, hydrated radii and ionic mobilities of Li^+, Na^+, K^+, Rb^+ and Cs^+ ions.

	Ion				
	Li^+	Na^+	K^+	Rb^+	Cs^+
Ionic radius (pm)[29]	76	102	138	152	167
Entalpy of hydratation (kJ mol^{-1})[30]	–520	–406	–322	–297	–276
Hydrated radius (pm)[29]	340	276	232	228	226
Ionic mobility (cm^2/Ω mol)[29]	33.5	43.5	64.5	67.5	68

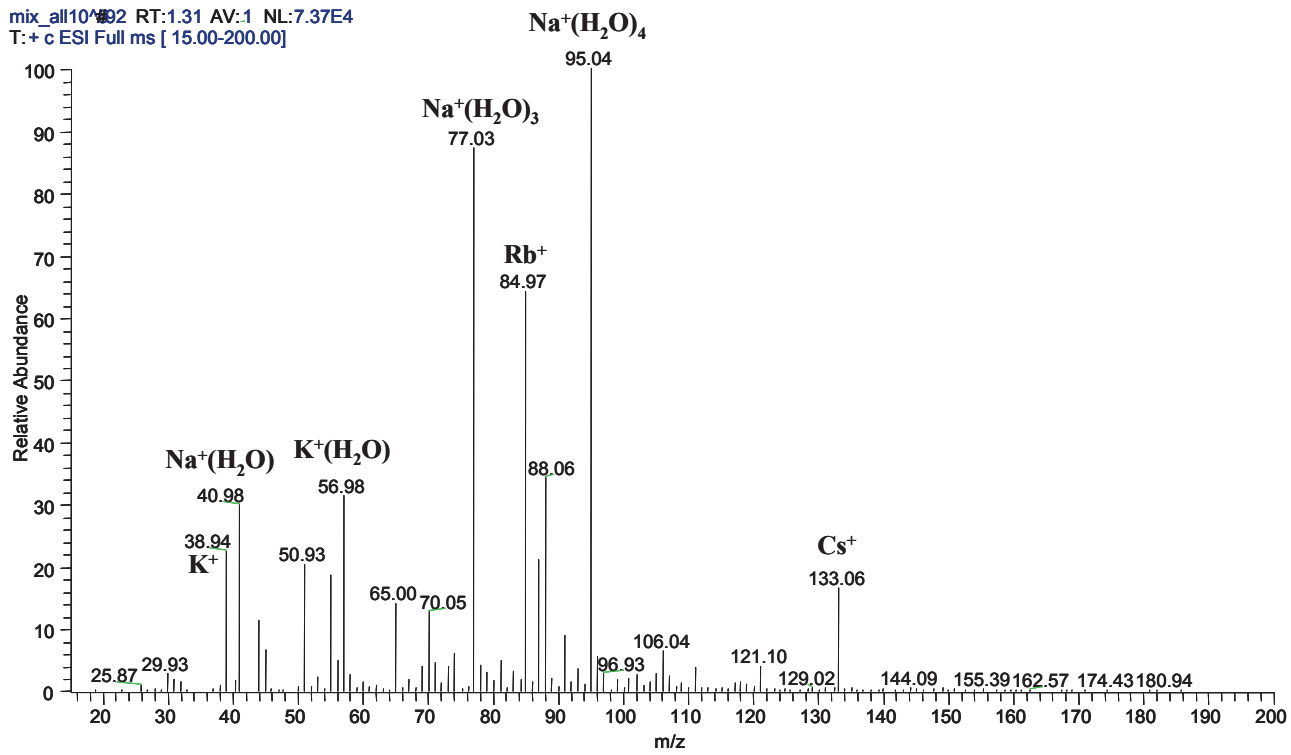

Figure 8. ESI mass spectrum of equimolar water solution of Na^+, K^+, Rb^+ and Cs^+.

In these conditions (V = 0.5 kV), the absolute intensities of Na^+, K^+, Rb^+ and Cs^+ would have to be, in principle, the same. However, they were found to be 0, 133, 291 and 210, respectively. While K^+, Rb^+ and Cs^+ ions exhibit intensities of the same order of magnitude, the complete absence of any signal due to Na^+ ions is quite unexpected. However, it should be emphasized that, in water solution, alkali metal ions are solvated. As reported by Koneshan *et al.*,[28] an analogous trend is observed by considering ion mobilities as a function of the crystallographic radius, R (Å) calculated from their mean square displacement. This behavior has been explained by the hydration enthalpy of the ions, which are inversely dependent on their dimension (see Table 1).[29,30]

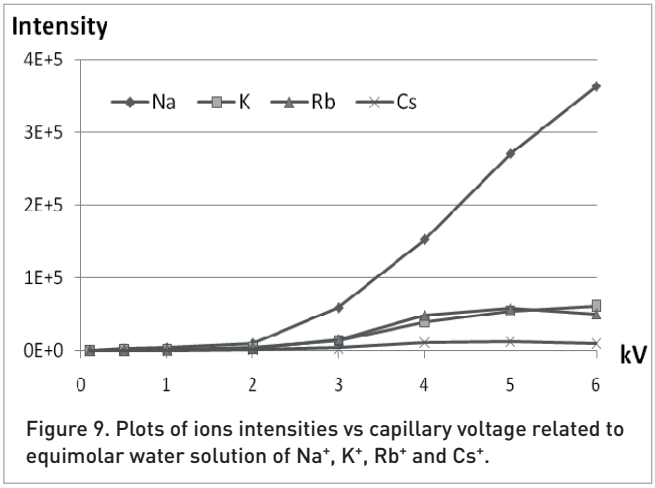

Figure 9. Plots of ions intensities vs capillary voltage related to equimolar water solution of Na^+, K^+, Rb^+ and Cs^+.

This aspect is confirmed by the spectrum (obtained for V = 0.5 kV) reported in Figure 8, in which hydrated Na^+ and K^+ ions are detectable. Considering the sum of intensities of the ions and their related water adducts, they become for Na^+ and K^+ of the same order of magnitude at 0.5 kV [Na^+ species]/[K^+ species] = [2625]/[1419], in agreement with the molar ratio [Na^+]/[K^+] = 1 in the original solution. By applying 4 kV on the spraying capillary, the ratio [Na^+ species]/[K^+ species] becomes [15,2941]/[39,942], which can be explained by the higher mobility of Na^+ species. It is interesting to observe (see Figure 8) that Na^+ is present only in hydrated form. The trend ion intensities vs capillary voltage is reported in Figure 9.

These results seem to indicate that the hypothesis on the possible inverse dependence of ion mobility vs ion mass and cross section is right: by increasing the capillary voltage, an increase in ion abundance, dependent on the ion mass and dimensions, is observed. It could be thought that the increase in ion abundance could be explained by better ion focalization along the final part of the capillary axis due to the ESI phenomena described above, but the higher abundance increase specifically observed for the smallest ions are a good indication that ion mobility also plays a role. This effect can also be present in the sprayed droplet, as described by Zhou and Cook[20] and, consequently, what was observed can be considered due to ion mobility phenomena occurring either in the capillary or in the sprayed droplet.

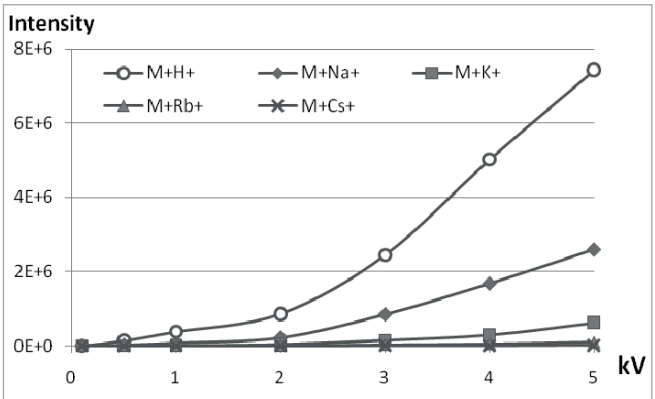

Figure 10. Plots of ion intensities vs capillary voltage related to water solution of AT2 dissolved in equimolar solution of Na^+, K^+, Rb^+ and Cs^+.

The different abundance of alkali cations, originating from their different ion mobility, leading to their different concentration, would necessarily reflect on the formation of cationized ions of analytes in different yields. The equimolar solution of Na^+, K^+, Rb^+ and Cs^+ was used as solvent for Angiotensin II (AT2) and spectra were recorded at different capillary voltages. The obtained results are reported in Figure 10. Of course, in this case, the most abundant species is MH^+, due to the higher concentration of H_3O^+ ions, but the abundance of MNa^+, MK^+, MRb^+ and MCs^+ ions are directly related to the observed abundance of the alkali ions. One point needs to be discussed. At 0.5 kV, the ion intensities of MH^+, MNa^+ and MK^+ are 136,378, 25,882 and 3693, respectively. In the absence of analyte, Na^+ ions are undectable (Figure 8). The data obtained in the presence of AT2 show that Na^+, as well as its hydrated species, are available to cationize the protein. Also, in this case, the concurrency of ion mobility phenomena occurring in both spraying capillary and sprayed droplets can explain the obtained results.

The above described behavior can be employed to explain some discrepancies between potenziometric and ESI data in the study of metal–ligand complexation.[31] In an investigation on the complexation of Al(III) with 1,6-dimethyl-4-hydroxy-3-pyridincarboxilic acid, the ratio $[AlL_3H]^+$ and $[AlL_2]^+$ was found to be practically unitary by the potenziometric measurements. The same solution,

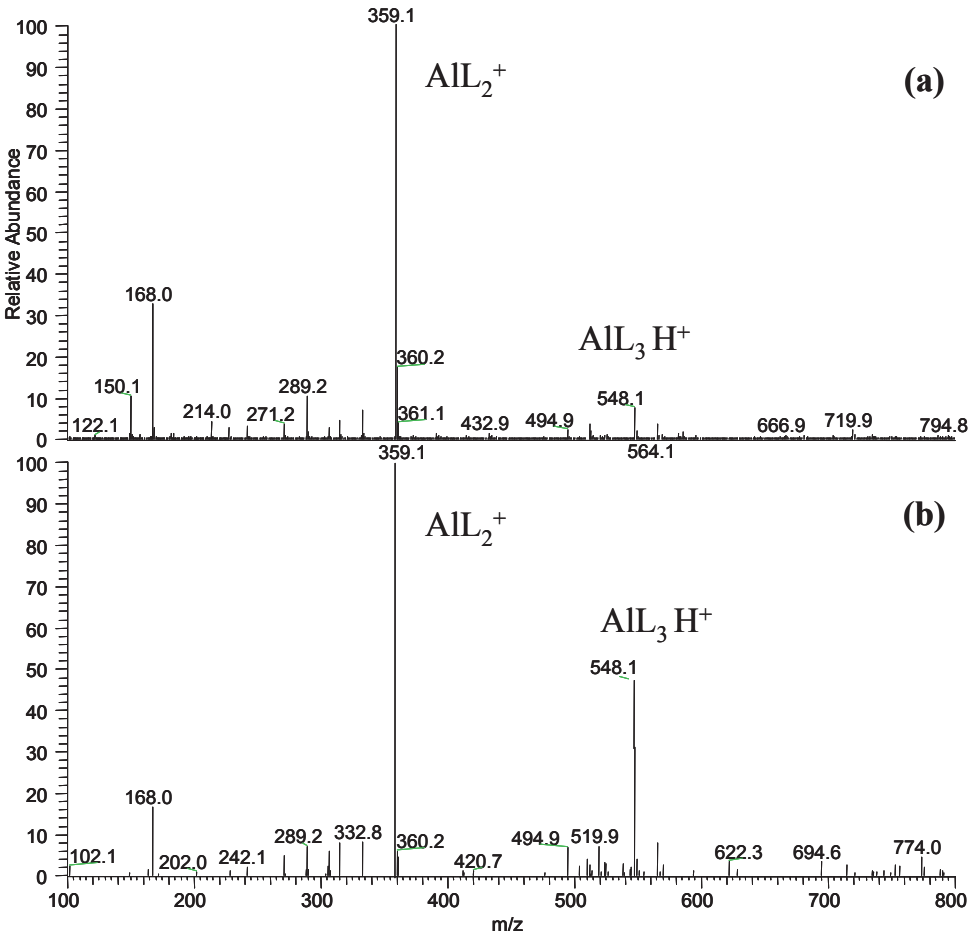

Figure 11. ESI mass spectra of the water solution of $AlCl_3$ and 1,6-dimethyl-4-hydroxy-3-pyridincarboxilic acid (L) (molar ratio 1:3) recorded at different capillary voltages: (a) 4 kV and (b) 0.1 kV.

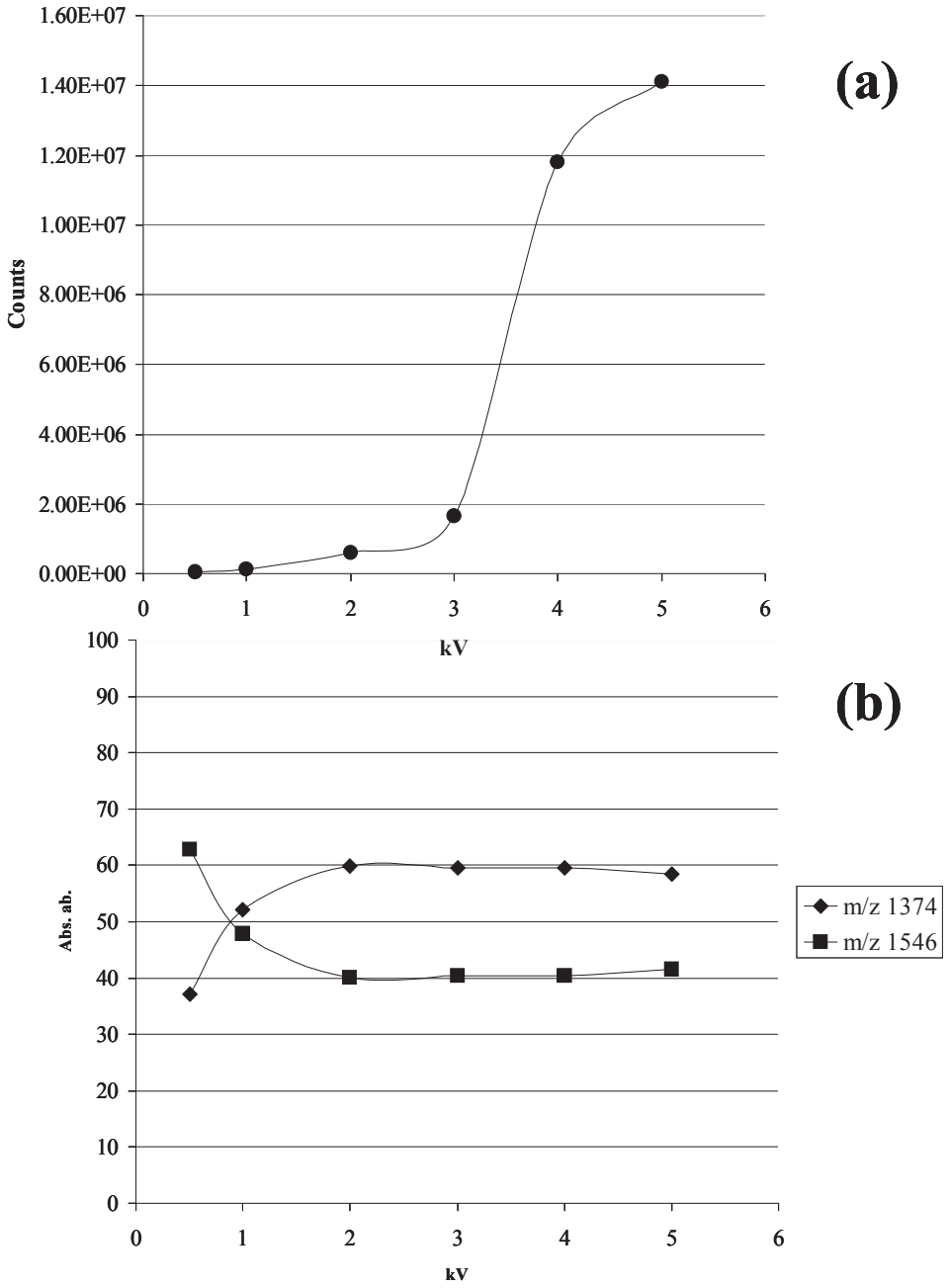

Figure 12. Total ion current vs capillary voltage of water solution of Cyt*C*.

when analyzed by ESI, led to the spectrum reported in Figure 11(a). The ratio between $[AlL_2]^+$ and $[AlL_3H]^+$ is about 20. This can be explained by different ion mobility of the two ions. In fact, by calculating by Gaussian 03W[32] the mean molecular radius, it is 1.0 nm for AlL_2^+ and 1.3 nm for AlL_3H^+. These values lead to a speed of 4.2 cm s^{-1} and 3.3 cm s^{-1}, respectively. Then AlL_2^+, being faster, reaches the apex of the Taylor cone more rapidly and its concentration is consequently increased. The opposite is valid for AlL_3H^+ ions. To verify this hypothesis, the solution was sprayed at a capillary voltage of 0.1 kV, i.e. far from the electrospray conditions. The spectrum obtained is reported in Figure 11(b). As can be observed, in these conditions the $[AlL_2]^+/[AlL_3H]^+$ abundance ratio shows a clear decrease, proving the perturbative effect of the ESI conditions.

Finally, to test the influence of charge state on ion mobility, some experiments were carried out on the ESI-generated, multi-charged species from Horse Heart Cytochrome *C* (Cyt*C*, MW: 12384 Da). The total ion current (TIC) due to molecular cluster (multi-charged species) vs capillary voltage shows the trend reported in Figure 12(a). As expected, a clear increase in TIC is observed by increasing the capillary voltage. However, a change in the relative abundance of differently charged species

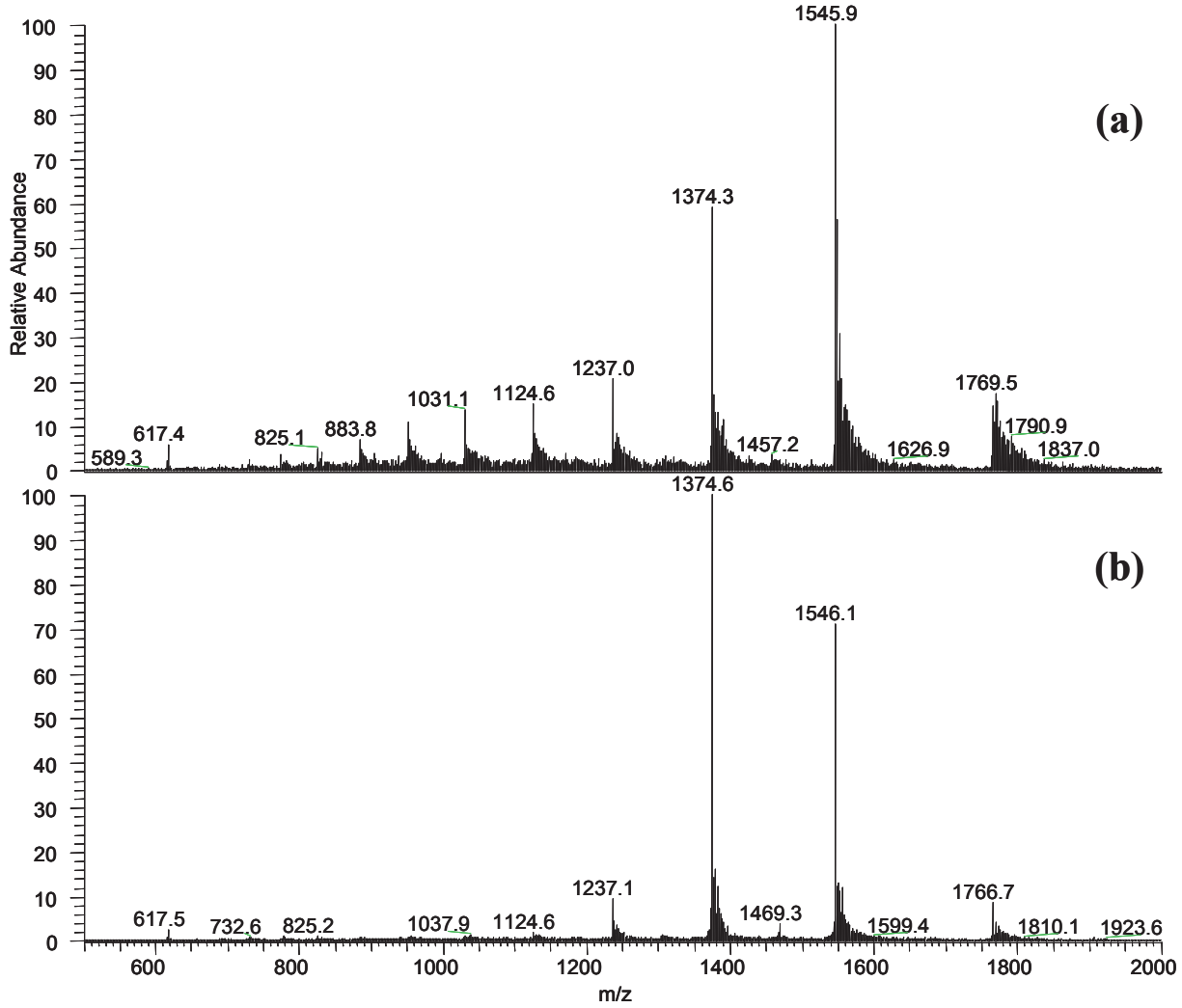

Figure 13. ESI mass spectra of water solution of Cyt*C* recorded at different capillary voltages: (a) 0.5 kV and (b) 5 kV.

is observed. At 0.5 kV, the most abundant ion is at *m/z* 1546, corresponding to $[M+8H]^{8+}$, while the $[M+9H]^{9+}$ ions at *m/z* 1374 show an abundance of 59% of the former. If ion mobility should play some role, an increase in relative abundance of the higher charged species by increasing the capillary voltage should be observed and the experimental data [Figure 12(b)] fully confirm this aspect. Alternatively, it could be proposed that the observed abundance increase could be due to a higher protonation reaction yield, due to the voltage increase. However, this hypothesis seems to be in contrast to the experimental data: the spectra obtained at 0.5 kV and 5 kV are reported in Figure 13. As it can be seen, higher charged states are present in the former case, while the results are suppressed in the presence of high voltage. This can be explained by a higher protonation yield of the most stable species: if this is true, the observed results could indicate that the $[M+9H]^{9+}$ species is energetically more favored than the $[M+8H]^{8+}$ species. However, the inversion of relative abundances cannot be fully explained by this view. Our impression is that both ion stability and ion mobility participate in the observed behavior.

In order to evaluate the role of ion mobility phenomena occurring in the sprayer capillary and in the ejected droplets some

Table 2. Geometrical parameters, applied voltages and electrical field calculated by the Loeb equation [Equation (8)] for the ESI and nanoESI sources.

Source	r_c	d	V	E_c
ESI	95 mm	0.25 cm	4 kV	1.89×10^5 V m^{-1}
nanoESI	20 mm	0.71 cm	1.9 kV	2.61×10^5 V m^{-1}

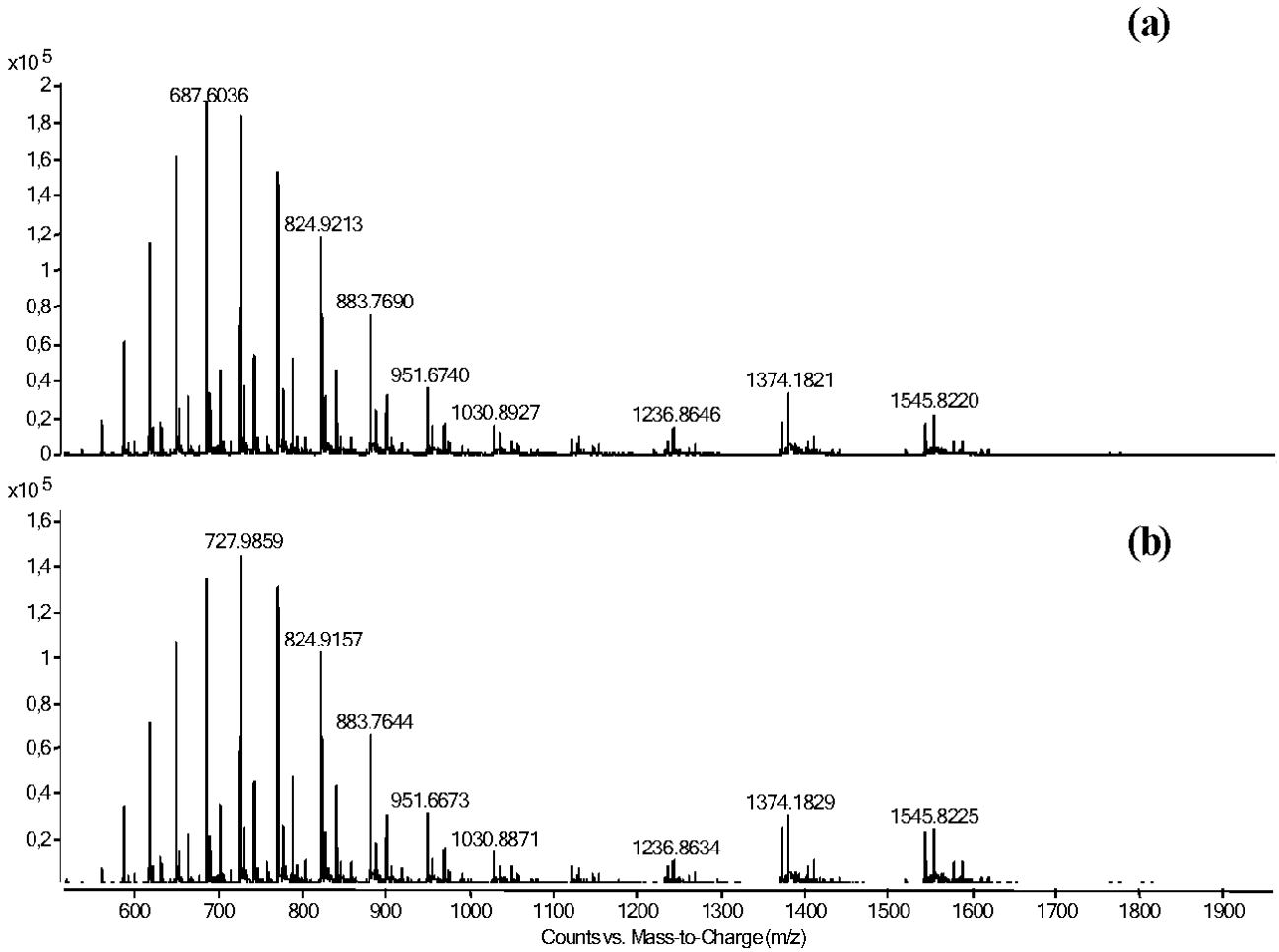

Figure 14. Mass spectra obtained in nanoESI conditions of water solution of Cyt*C* recorded at different entrance capillary voltages: (a) 1.9 kV and (b) 1.72 kV.

further experiments on Cyt*C* were performed in nanoESI conditions. The geometrical parameters and the applied voltages of ESI and nanoESI sources are reported in Table 2, together with the electrical field present at the capillary tip [calculated by Equation (8)]. As can be seen, the geometrical parameters and the applied voltages lead to an electrical field of the same order of magnitude. The possible differences observed between the experiments carried out in the two operative conditions can lie in the droplet dimensions. The spectra obtained in nanoESI conditions, with applied voltages of 1900 V and 1720 V, are reported in Figures 14(a) and (b), respectively (for higher and lower voltages the source did not work properly). These spectra are very different from those obtained by ESI (Figure 13). In nanoESI spectra, the ions at *m/z* 1546, *m/z* 1374 and *m/z* 1237 are still present, but the most abundant ions are detected in the range of *m/z* values 590–1000, corresponding to $[M+21H]^{21+}$–$[M+13H]^{13+}$. The same ions were virtually absent in the ESI spectra. By decreasing the applied voltage from 1.9 kV to 1.72 kV, some minor changes in the relative abundance of multicharged ions are observed. These results seem to indicate that in nanoESI conditions, due to the smallest droplet dimension and to the smallest internal diameter of the spraying capillary, ion mobility phenomena play a major role in the sprayed droplets with the privileged detection of highly charged species.

In conclusion, the obtained results indicate that the ion mobility of the ions present in the sprayed solution surely affects the ESI measurements. Ions of smaller dimension and/or higher charge state exhibit higher abundances and this behavior can be carefully taken into account in ESI measurements and invoked to explain the ion suppression phenomenon often observed in ESI experiments.

References

1. R.B. Cole, *Electrospray and MALDI Mass Spectrometry: Fundamentals, Instrumentation, Practicalities and Biological Applications.* John Wiley & Sons, Inc., Hoboken, New Jersey, USA (2010).
2. M. Yamashita and J.B. Fenn, "Electrospray ion source. Another variation on the free-jet theme", *J. Phys. Chem.* **88,** 4451 (1984). doi: 10.1021/j150664a002

3. P. Kebarle and U.H. Verkerk, "Electrospray: From ions in solution to ions in the gas phase, what we know now", *Mass Spectrom. Rev.* **28,** 898 (2009). doi:10.1002/mas.20247
4. Oak Ridge National Laboratory, *Review, State of the Laboratory*, Vol. 29 no.1/2. Oak Ridge National Laboratory, Tennessee, USA (1995).
5. J.N. Smith, *Fundamental Studies of Droplet Evaporation and Discharge Dynamics in Electrospray Ionization*. California Institute of Technology, California, USA, 303 pp. (2000).
6. J. Zeleny, "Instability of electrified liquid surfaces", *Phys. Rev.* **10,** 1 (1917). doi: 10.1103/PhysRev.10.1
7. G. Taylor, "Disintegration of water drops in an electric field", *Proc. R. Soc. London, Ser. A* **280,** 383 (1964). doi: 10.1098/rspa.1964.0151
8. G. Taylor, "Studies in Electrohydrodynamics. I. The Circulation Produced in a Drop by Electrical Field", *Proc. R. Soc. London, Ser. A* **291,** 159 (1966). doi: 10.1098/rspa.1966.0086
9. R.L. Hines, "Electrostatic atomization and spray painting", *J. Appl. Phys*. **37,** 2730 (1966). doi: 10.1063/1.1782112
10. R. Tilney, "Electrostatic coating processes", *Brit. J. Appl. Phys*. **4,** S51 (1953). doi: 10.1088/0508-3443/4/S2/321
11. M. Dole, L.L. Mack, R.L. Hines, R.C. Mobley, L.D. Ferguson and M.B. Alice, "Molecular beams of macroions", *J. Chem. Phys.* **49,** 2240 (1968). doi: 10.1063/1.1670391
12. A.T. Blades, M.G. Ikonomou and P. Kebarle, "Mechanism of electrospray mass spectrometry. Electrospray as an electrolysis cell", *Anal. Chem.* **63,** 2109 (1991). doi: 10.1021/ac00019a009
13. R.J. Pfeifer and C.D. Hendricks, Jr, "Parametric studies of electrohydrodynamic spraying", *AIAA J.* **6,** 496 (1968).
14. J.F. de la Mora and I.G. Loscertales, "The current emitted by highly conducting Taylor cones", *J. Fluid Mech*. **260,** 155 (1994). doi: 10.1017/S0022112094003472
15. L. Rayleigh, "On the equilibrium of liquid conducting masses charged with electricity", *Philos. Mag.* **14,** 184 (1882). doi: 10.1080/14786448208628425
16. M. Peschke, U.H. Verkerk and P. Kebarle, "Features of the ESI mechanism that affect the observation of multiply charged noncovalent protein complexes and the determination of the association constant by the titration method", *J. Am. Soc. Mass Spectrom.* **15,** 1424 (2004). doi: 10.1016/j.jasms.2004.05.005
17. R.B. Cole, "Some tenets pertaining to electrospray ionization mass spectrometry", *J. Mass Spectrom*. **35,** 763 (2000). doi: 10.1002/1096-9888(200007)
18. P. Kebarle and M. Peschke, "On the mechanisms by which the charged droplets produced by electrospray lead to gas phase ions", *Anal. Chim. Acta* **406,** 11 (2000). doi: 10.1016/S0003-2670(99)00598-X
19. B.A. Thomson and J.V. Iribarne, "Field induced ion evaporation from liquid surfaces at atmospheric pressure", *J. Chem. Phys.* **71,** 4451 (1979). doi: 10.1063/1.438198
20. S. Zhou and K.D. Cook, "A mechanistic study of electrospray mass spectrometry: charge gradients within electrospray droplets and their influence on ion response", *J. Am. Soc. Mass Spectrom.* **12,** 206 (2001). doi: 10.1016/S1044-0305(00)00213-0
21. R.L. Grimm and J.L. Beauchamp, "Dynamics of field-induced droplet ionization: time-resolved studies of distorsion, jetting and progeny formation from charged and neutral methanol droplets exposed to strong electric field", *J. Phys. Chem. B* **109,** 8244 (2005). doi: 10.1021/jp0450540
22. A. Gomez and K. Tang, "Charge and fission of droplets in electrostatic sprays", *Phys. Fluids* **6,** 404 (1994). doi: 10.1063/1.868037
23. L. Loeb, A.F. Kip, G.C. Hudson and W.H. Bennet, "Pulses in negative point-to-plane corona" *Phys. Rev.* **60,** 714 (1941). doi: 10.1103/PhysRev.60.714
24. R. Rellán-Álvarez, J. Abadía and A. Álvarez-Fernandez, "Formation of metal-nicotianamine complexes as affected by pH, ligand exchange with citrate and metal exchange. A study by electrospray ionization time-of-flight mass spectrometry", *Rapid Commun. Mass Spectrom.* **22,** 1553 (2008). doi: 10.1002/rcm.3523
25. L. Tang and P. Kebarle, "Dependence of ion intensity in electrospray mass spectrometry on the concentration of the analytes in the electrosprayed solution", *Anal. Chem.* **65,** 3654 (1993). doi: 10.1021/ac00072a020
26. H.D. Beckey, *Field Ionization Mass Spectrometry*. Pergamon Press, Oxford, UK (1971).
27. D.P.H. Smith, "The electrohydrodynamic atomization of liquids", *IEEE Trans. Ind. Appl*. **22,** 527 (1986). doi: 10.1109/TIA.1986.4504754
28. S. Koneshan, J.C. Rasaiah, R.M. Lynden-Bell and S.H. Lee, "Solvent structure, dynamics, and ion mobility in aqueous solutions at 25°C", *J. Phys. Chem.* **102,** 4193 (1998). doi: 10.1021/jp980642x
29. http://www.tutorvista.com/content/chemistry/chemistry-iii/s-block-elements/alkali-metals.php
30. http://chemistry.uwaterloo.ca/~cchieh/cact/tools/hydrationegy.html
31. V. Di Marco *et al.*, results to be published.
32. www.gaussian.com

Padova—Prato della Valle square and Santa Giustina Church

Padova—The "Specola" from which Galileo observed the stars.

Venice—Resotration leaves unaltered Venice atmosphere.

Venice—A houseboat at Riva degli Schiavoni.

MS group of CNR/ISTM in Padova. From left to right: Giacomo Ricci, Giulio Vacilotto, Enrico Boscaro, Laura Rebecchi, Simona Porcu, Sara Crotti, Pietro Traldi, Roberta Seraglia, Laura Molin, Federico Bordin, Floriana Moiseenco, Ilena Isak.